4. COSMIC DISTANCES AND STRUCTURES

Matthew Baring – Lecture Notes for ASTR 360, Spring 2025

1 Distance Determinations

• Various techniques are employed by astronomers for distance determination. These include parallax and proper motion measurements on nearer scales, ranging out to supernovae indicators in the early universe. **C & O, Sec. 27.1**

∗ Main sequence fitting using the Hertzsprung-Russell diagram and luminosity class characteristics can be reliably used within the Milky Way;

∗ Cepheid variables' period-luminosity relation, calibrated using parallax measurements, extends out to nearby galaxies (i.e. 5 Mpc);

∗ Calibrated luminosity functions for certain populations such as globular clusters can probe out to the 100 Mpc distance scale;

Plot: Globular Cluster Luminosity Function

∗ The Tully-Fisher law $d_{\rm TF} \propto v_c^{9/4}/\mathcal{F}^{1/2}$ can be applied out to 100 Mpc, and SNIa standard candle light curves can probe beyond $z \sim 1$.

Plot: Extragalactic and Cosmological Distance Determination Techniques

• Many of these techniques employ distance moduli using local benchmark calibrations of given populations of sources. This underlines the importance of distance calibration astrometry missions such as *Hipparcos* and *Gaia*.

Globular Cluster Luminosity Function

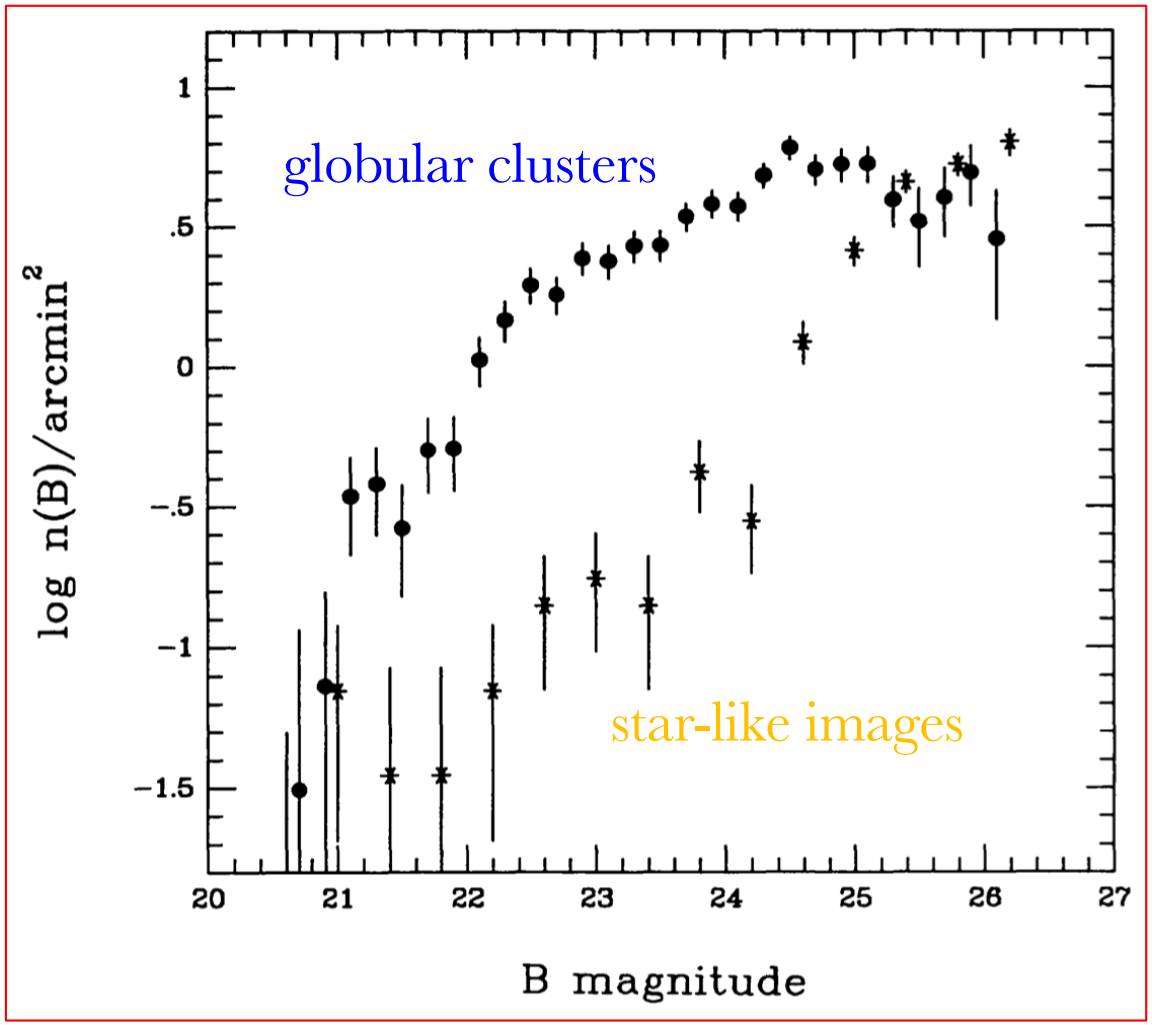

Harris et al., ApJ Supp. **76**, 115 (1991)

- Luminosity function (LF) for globular clusters around 4 giant elliptical galaxies in the Virgo cluster (d=16 Mpc).
- Uses CCD photometry.
- Observe the "peak" at around $m_B \sim 25$, which doesn't exist for the LF for field galaxies.
- The stars represent the counts of star-like images in the galaxy fields; a contaminant.
- This shape can be compared with those of more distant galaxy clusters to derive their approximate distances.

Cosmological Distance Ladder - from Rowan-Robinson (1985)

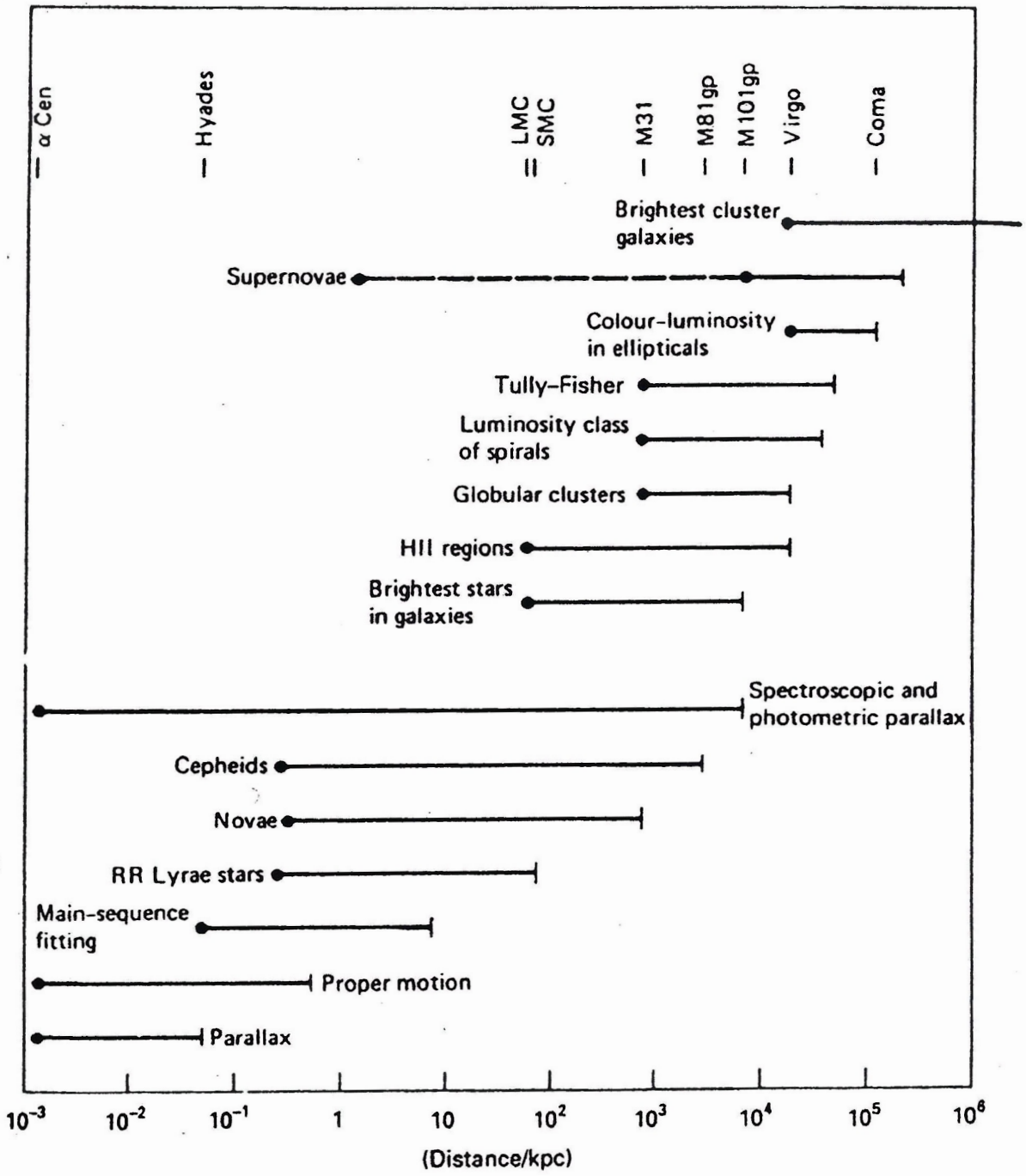

Fig. 8.2. Illustrating the 'cosmological distance ladder' (after Rowan-Robinson 1985). The diagram shows the range of distances over which different classes of object can be used to estimate the astronomical distances.

2 Hubble's Law

• Edwin Hubble observed in 1929 that galaxies were on average receding from Earth, and that their velocities v as inferred from **spectroscopic redshifts** z were proportional to their distance d (in Mpc) away: **C & O, Sec. 27.2**

$$v \;=\; H_0\, d \quad , \tag{1}$$

where H_0 is **Hubble's constant**. The spectroscopic redshift z and velocity are related via $v/c = \mathrm{z} = \lambda_{obs}/\lambda_{emit} - 1$. **Longair, Sec. 2.2**

$*$ Based on a very limited *local* sample, Hubble deduced the value $H_0 = 550$ km/sec/Mpc, a value grossly over-estimating the current determination. In Hubble's time, higher redshift galaxies were observed to be less luminous on average; now we have more reliable distance indicators.

Plot: Hubble Expansion: Historical Perspective

• Sandage (1958) refined this dramatically using clusters out to $z \sim 0.5$, yielding 50 km/sec/Mpc $< H_0 <$ 100 km/sec/Mpc. This served as the status quo until the 1990s.

• In the 1990s, Hipparcos astrometry refined the local distance standard to yield an improvement in the precision of the H_0 determination:

$$\boxed{\boxed{H_0 \;=\; 75 \pm 15 \mathrm{km/sec/Mpc} \quad .}} \tag{2}$$

Hubble's law can be expressed in observer-friendly units using apparent magnitudes, the common form for its observational expression:

$$\boxed{\log_{10} z \;=\; 0.2(m - M) - 5 + \log_{10}(H_0/c \times 1\mathrm{Mpc}) \quad .} \tag{3}$$

This is a distance modulus form. N.B. Magnitude has limitations as a distance indicator due to spread in the source luminosity function $f(M)$.

Hubble's Expansion Law

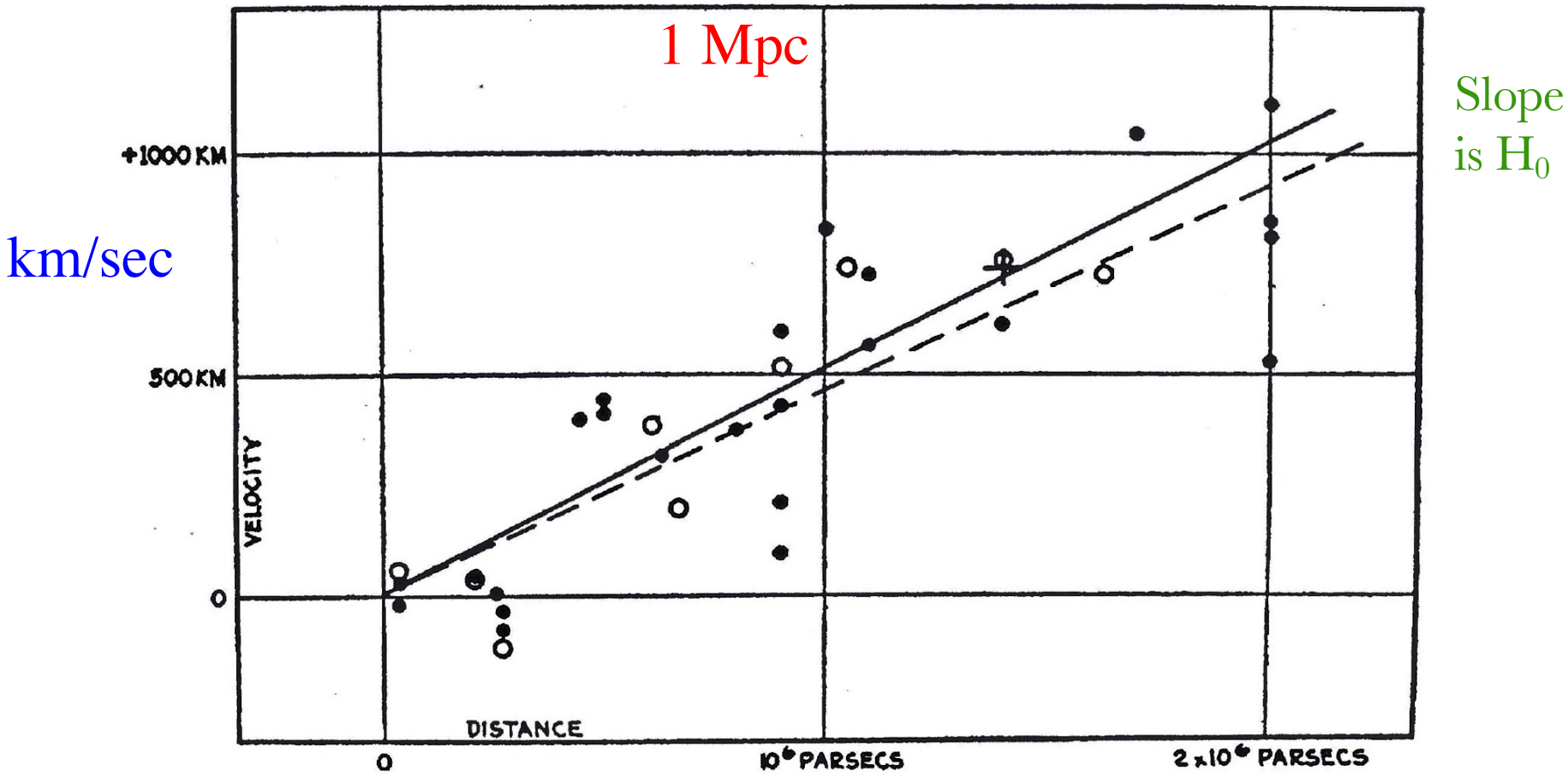

- Hubble's 1936 velocity-distance relation for 32 galaxies. The two lines use different corrections for the sun's motion.

Accordingly, logarithmic redshift versus magnitude diagrams are *de rigueur* in the field. These are known as **Hubble diagrams**. Straight lines indicate flat spacetime and no source evolution.

Plot: Redshift-magnitude relation for radio and field galaxies

$*$ For the radio galaxies, the observed upward curvature in K magnitude at $z \gtrsim 1$ is as much of an indicator of luminosity evolution than spacetime curvature. It exhibits clearer evidence of high z effects.

$*$ For the field galaxies, the downward curvature (a fainter trend at high z) is evidence for spacetime curvature, though there are also source evolutionary influences in the mix. The huge scatter at low z reflects a greater relative contribution from peculiar velocities.

• N.B. The peculiar velocity of the local group is ~ 600 km/sec, inferred from the CMB dipole pattern; pinning down such a velocity prior to COBE (launched in 1990) was much more difficult.

• High z behavior provides evidence of the **Malmquist bias**, a luminosity sampling selection effect. Due to finite sampling down to some apparent magnitude, intrinsically brighter galaxies preferentially contribute at high z, whereas less luminous ones are missed. This skews the $m(z)$ shape a little, and must be corrected for in order to ascertain true $m(z)$ behavior.

$*$ Using better standard candles helps eliminate the Malmquist bias.

Plot: Various Hubble Constant Determinations

Redshift-Magnitude Relations

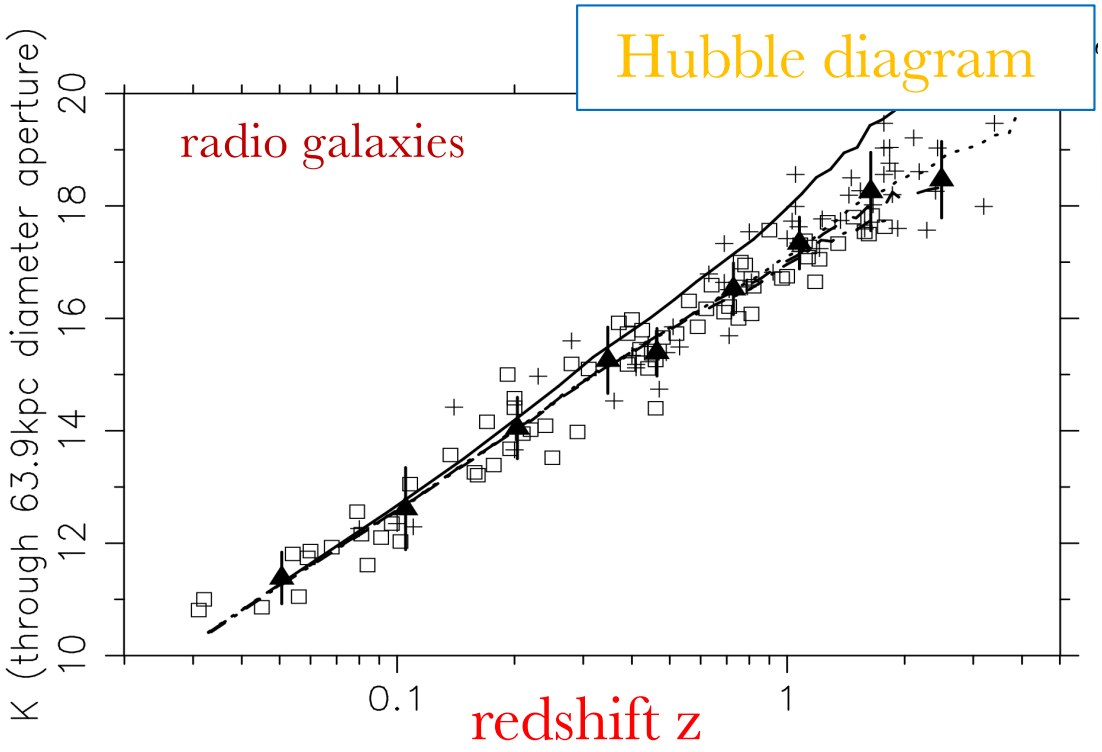

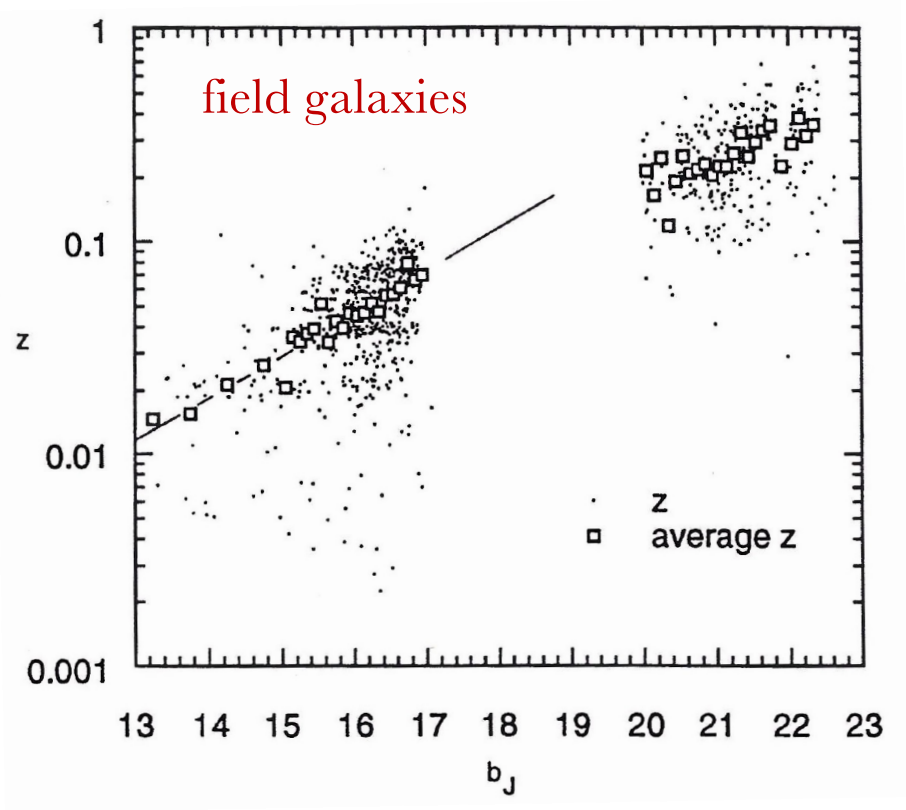

- *Left*: K-band (IR) redshift-magnitude (Hubble) diagram for radio galaxies (RGs). The cosmological model is a marginally-closed universe. Squares and crosses constitute different RG samples. Curves are models without (solid) and with source evolution. Figure 1 of Inskip et al. MNRAS **329**, 277 (2002).
- *Right*: redshift versus apparent magnitude for field galaxies (dots). Squares represent magnitude averages at fixed z. Note the swapped axes from the LHS. From Shanks (1991; see Peebles *Physical Cosmology*).

Hubble Constant Data

Method Used	Authors	Value, km/s/Mpc
Cepheid variables in distant galaxies	W. Freedman et al (1999)	70 +/- 7
M101 group velocity and distance	Sandage and Tammann (1974)	55.5 +/- 8.7
Virgo Cluster	Peebles (1977)	42 - 77
Globular Clusters	Hanes (1979)	80 +/- 11
Virgo Sc HII luminosities	Kennicutt (1981)	55
Type I supernovae	Branch (1979)	56 +/- 15
Type I supernovae	Sandage and Tammann (1982)	50 +/- 7
Infrared Tully-Fisher relation	Aaronson and Mould (1983)	82 +/- 10
SN-Ia and Cepheids	Sandage, et al. (1994)	55 +/- 8
Cepheids in Virgo (M100)	Freedman, et al. (1994)	80 +/- 17
Surface Brightness Fluctuation	Tully (1993)	90 +/- 10
Final Results from the Hubble Space Telescope Key Project to Measure the Hubble Constant	(2000) W. L. Freedman, B. F. Madore, B. K. Gibson, L. Ferrarese, D. D. Kelson, S. Sakai, J. R. Mould, R. C. Kennicutt, Jr., H. C. Ford, J. A. Graham, J. P. Huchra, S. M. G. Hughes, G. D. Illingworth, L. M. Macri, P. B. Stetson	72 +/- 8
In the February, 2003, the results of the first year of WMAP observations were released. (WMAP = Wilkinson Microwave Anisotropy Probe)	WMAP Science Team WMAP, CBI, ACBAR = WMAPext+2dF =	Different methods give values: 73 +/- 5 73 +/- 3

3 Supernova Surveys

• The best candidates for standard candles at moderate and high redshifts ($z > 0.1$) are **type Ia supernovae**, which come from CO white dwarfs. **C & O, pp. 1042-4**

SN Ia occur in binary star systems containing a white dwarf that accretes matter from its post main sequence companion. The companion is normally in a giant phase so that it permits **Roche lobe overflow**. The accretion ensues until the white dwarf mass approaches the Chandrasekhar mass limit of $1.4 M_\odot$. The dwarf then becomes unstable and explodes in the supernova event that we see. Since the mass range of progenitor white dwarfs is very narrow, the explosion physics drives a very constrained range of luminosities so that the SN Ia event is a **standard candle** to a fairly high degree.

∗ Hence, these supernovae are reliable distance indicators, and have been so used since 1995 in deep automated surveys as supernova cosmology probes. With essentially fixed L , they enable determination of curvature in $m(z)$, the apparent magnitude – redshift plot or **Hubble diagram**. This affords probes of key cosmological parameters such as Ω_m and Ω_Λ , to be discovered. **Longair, pp. 201-4**

∗ SN Ia are very bright, with typical luminosities $\gtrsim 10^{43}$ erg/sec (magnitudes $M \sim -19.5 \pm 0.6$), and so can be seen to redshifts $z \gtrsim 1$. Their light curve width couples to their luminosity, leading to a calibration correction.

Plot: SN Ia lightcurves

• Saul Perlmutter, Brian Schmidt and Adam Riess won the 2011 Nobel Prize in physics for their SN Ia cosmology work in demonstrating **cosmic acceleration** of the universe at $z \lesssim 2$.

∗ Their work was able to provide significant constraints on the density parameters that suggested that $\Omega \sim 1$, and $\Omega_\Lambda \sim 0.7$ with $\Omega_m \sim 0.3$ (including dark matter). The cosmic density phase space was further constrained by the precision CMB results of WMAP and Planck, and the modern Dark Energy Survey SNIa supernova initiative.

Plot: Dark Energy Survey Hubble Diagram

SNIa Light Curves

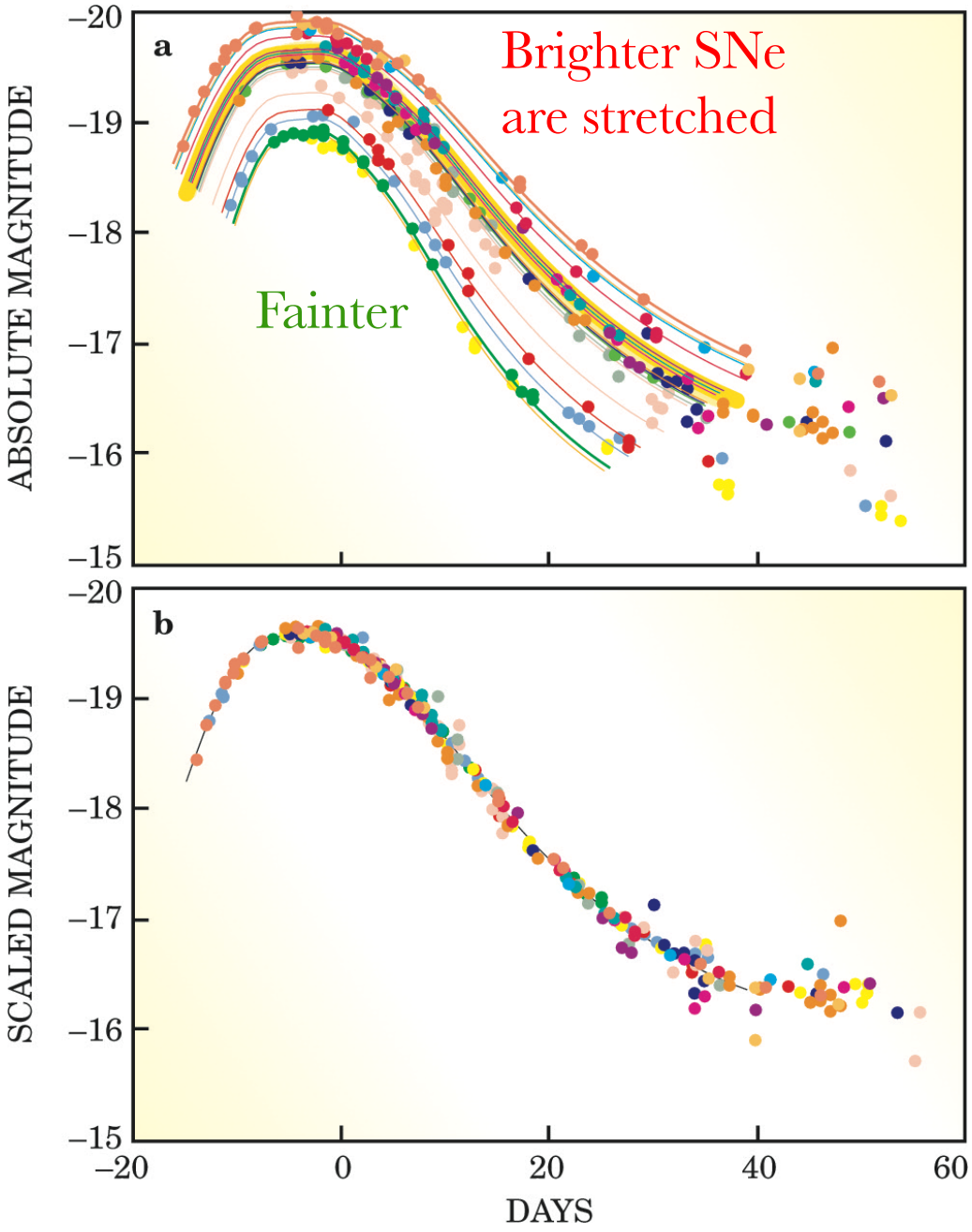

- Light curves before and after peak light for relatively nearby type Ia supernovae, represented in the star's rest frame (top).
- Most LCs lie in the yellow band.
- The brighter SNIa have stretched light curves, likely a consequence of explosion physics.
- By stretching the time scales of individual light curves to fit the norm, and scaling the brightness by an amount required by the time stretch, all the type Ia light curves match (bottom).

Perlmutter, *Physics Today*, **56**, 53 (2003)

Dark Energy Survey Hubble Diagram

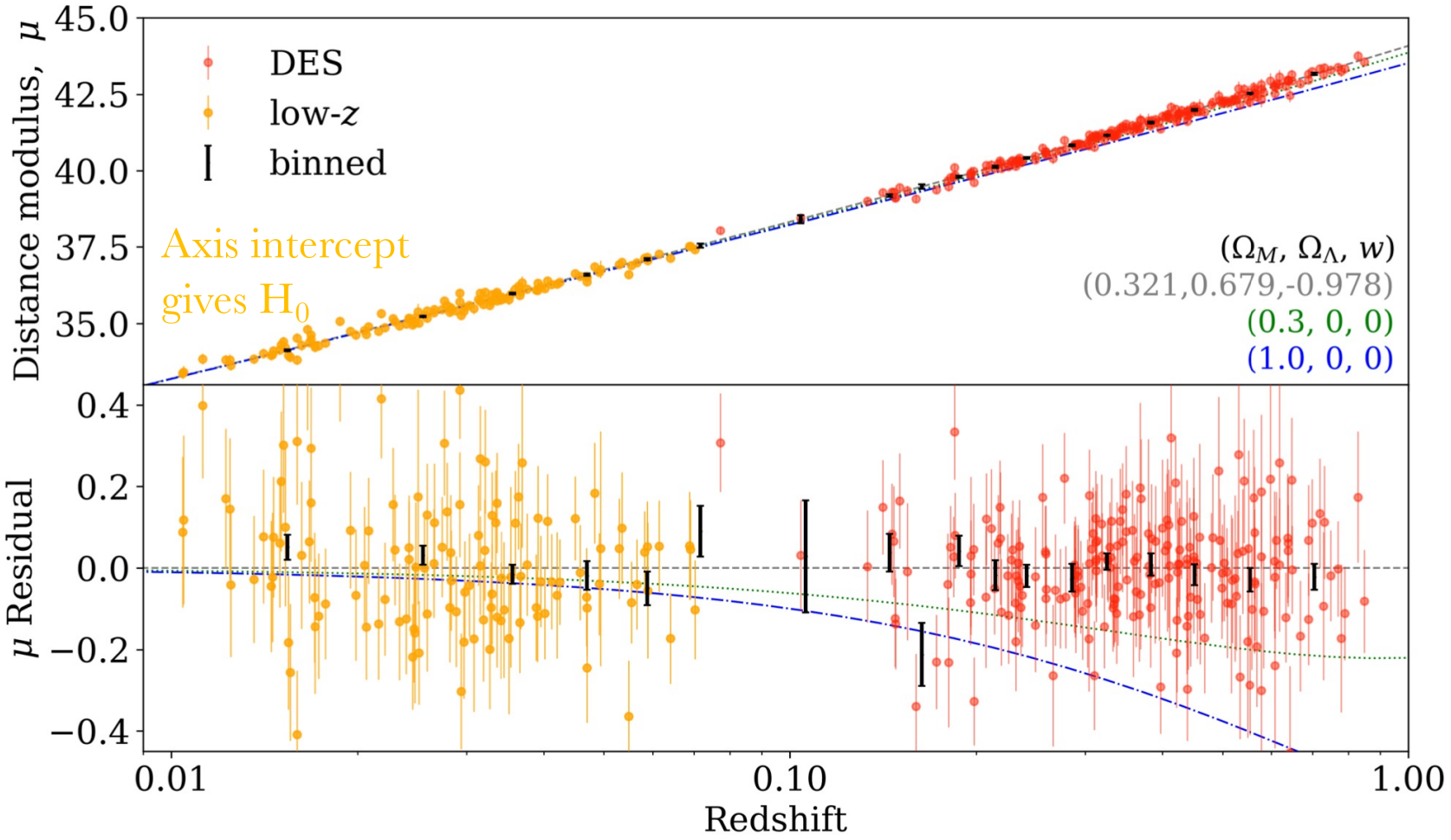

- Distance modulus (a proxy for apparent magnitude) for 329 SNIae from DES 3 year data release. Three cosmological models are shown, with residuals.
- Abbott et al. ApJL **872**, L30 (2019).